

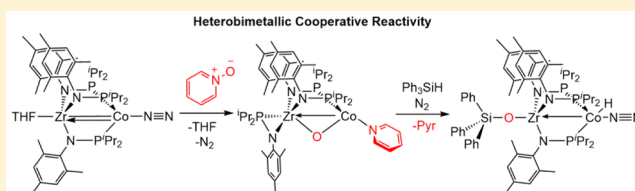
# Formation and Subsequent Reactivity of a N<sub>2</sub>-Stabilized Cobalt–Hydride Complex

Jeremy P. Krogman, Bruce M. Foxman, and Christine M. Thomas\*

Department of Chemistry, Brandeis University, 415 South Street MS 015, Waltham, Massachusetts 02454, United States

## Supporting Information

**ABSTRACT:** The reduced heterobimetallic Co/Zr complex N<sub>2</sub>Co(<sup>i</sup>Pr<sub>2</sub>PNMes)<sub>3</sub>Zr(THF) (**1**) has been previously reported to react with the C=O bonds of CO<sub>2</sub> and benzophenone to generate Zr/Co μ-oxo complexes OC-Co(<sup>i</sup>Pr<sub>2</sub>PNMes)<sub>2</sub>(μ-O)Zr(<sup>i</sup>Pr<sub>2</sub>PNMes) (**1-CO<sub>2</sub>**) and Ph<sub>2</sub>C=Co(<sup>i</sup>Pr<sub>2</sub>PNMes)<sub>2</sub>(μ-O)Zr(<sup>i</sup>Pr<sub>2</sub>PNMes) (**1-Ph<sub>2</sub>CO**), respectively. Herein, we report a similar reaction of **1** with pyridine-*N*-oxide to form an analogous complex (pyridine)<sub>2</sub>Co(<sup>i</sup>Pr<sub>2</sub>PNMes)<sub>2</sub>(μ-O)Zr(<sup>i</sup>Pr<sub>2</sub>PNMes) (**2**) with a more labile ligand bound to cobalt. Much like **1-CO<sub>2</sub>** and **1-Ph<sub>2</sub>CO**, compound **2** reacts with Ph<sub>3</sub>SiH via formation of a Si–O linkage to form (N<sub>2</sub>)(H)Co(<sup>i</sup>Pr<sub>2</sub>PNMes)<sub>3</sub>ZrOSiPh<sub>3</sub> (**5**). The dinitrogen ligand in **5** is weakly bound and can be readily removed in vacuo or displaced by other L-type ligands. This allows complex **5** to undergo insertion reactions with unsaturated substrates, including diphenyldiazomethane, CO<sub>2</sub>, benzonitrile, and phenylacetylene to give hydrazonato (Ph<sub>2</sub>C=NNH)Co(<sup>i</sup>Pr<sub>2</sub>PNMes)<sub>3</sub>ZrOSiPh<sub>3</sub> (**7**), formate (OC(H)O)Co(<sup>i</sup>Pr<sub>2</sub>PNMes)<sub>3</sub>ZrOSiPh<sub>3</sub> (**8**), ketimide (PhHC=N)Co(<sup>i</sup>Pr<sub>2</sub>PNMes)<sub>3</sub>ZrOSiPh<sub>3</sub> (**9**), and ylide Co(PhHC=CHP<sup>r</sup>Pr<sub>2</sub>NMes)(<sup>i</sup>Pr<sub>2</sub>PNMes)<sub>2</sub>ZrOSiPh<sub>3</sub> (**10**) products, respectively. Compound **5** was also found to catalyze the isomerization of 1-hexene to internal isomers.



## INTRODUCTION

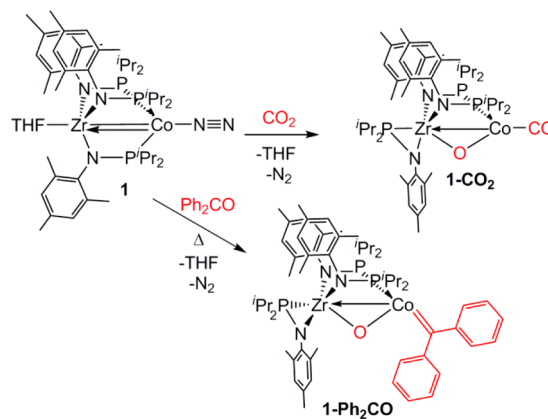
Complexes having metal–metal multiple bonds have been of fundamental interest for more than 50 years. Although the majority of such compounds have been homometallic systems,<sup>1</sup> heterobimetallic complexes that exploit the combination of an early and late transition metal to engender cooperative reactivity patterns have become a particular area of interest.<sup>2</sup> Motivation to study discrete early/late heterobimetallic compounds originally stemmed from phenomena observed in heterogeneous catalysis. In 1978, Tauster first invoked metal–metal interactions, termed “strong metal–support interactions” (SMSIs), in titania-supported noble metal catalysts to explain discrepancies between metal particle sizes measured by chemisorption and X-ray diffraction methods.<sup>3</sup> Since this seminal report, SMSIs have been implicated in promoting the activity of Fischer–Tropsch and CO<sub>2</sub>–CH<sub>4</sub> re-forming catalysts.<sup>4</sup> Strong metal–support interactions are generally invoked for a reducible support (e.g., TiO<sub>2</sub>), and in some cases, the formation of SMSIs or even bona fide metal–metal bonds have been found to be reversible by alternating reduction/oxidation processes.<sup>5</sup>

In an effort to mimic SMSIs using well-defined homogeneous model complexes, early/late heterobimetallic complexes and their reactivity have been investigated.<sup>2</sup> Our group has recently been focusing on phosphinoamide-supported metal–metal interactions in early/late heterobimetallic complexes, as well as their redox properties and reactivity toward the activation of both  $\sigma$  and  $\pi$  bonds in small-molecule substrates.<sup>6</sup> A Co/Zr heterobimetallic complex N<sub>2</sub>Co(<sup>i</sup>Pr<sub>2</sub>PNMes)<sub>3</sub>Zr(THF) (**1**) featuring a tris(phosphinoamide) ligand set has been shown

to form a short metal–metal triple bond, comprising one  $\sigma$  and 2 $\pi$  bonds from a dative Co→Zr interaction, upon reduction.<sup>6b,7</sup>

This bond formation is reversible, and the metal–metal bond is cleaved upon oxidation. The reaction of **1** with CO<sub>2</sub> and benzophenone exemplifies such a two-electron redox event (Scheme 1). Upon loss of the N<sub>2</sub> ligand from **1**, the C=O bond of CO<sub>2</sub> or benzophenone can be oxidatively added across the Co→Zr multiple bond to give **1-CO<sub>2</sub>** and **1-Ph<sub>2</sub>CO**, respectively.<sup>6d,8</sup> While these reactions are of interest in their own right, further reactivity of **1-CO<sub>2</sub>** and **1-Ph<sub>2</sub>CO** is thwarted

## Scheme 1



Received: March 4, 2015

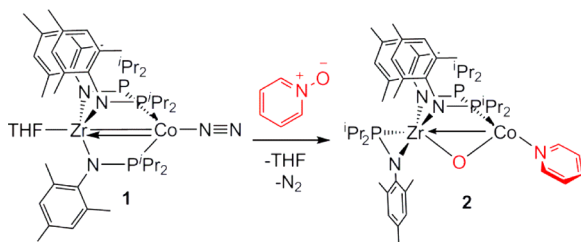
Published: June 25, 2015

by both strong Zr–O linkages and tight binding of the CO and carbene ligands to cobalt. Continuing these studies, we explore herein an analogous two-electron oxidation of **1** with pyridine-*N*-oxide to form a Co/Zr  $\mu$ -oxo complex with a more labile pyridine ligand on cobalt. The further reactivity of the resulting compound with Si–H bonds is explored and compared to that of **1-CO<sub>2</sub>** and **1-Ph<sub>2</sub>CO**, uncovering a well-defined low-coordinate cobalt(I)–hydride complex with a weakly bound N<sub>2</sub> ligand. The new cobalt–hydride complex is interesting given the important role that cobalt–hydride complexes play in reactions such as CO<sub>2</sub> hydrogenation,<sup>9</sup> hydroformylation,<sup>10</sup> electrocatalytic hydrogen evolution,<sup>11</sup> and catalytic organometallic transformations.<sup>12</sup> The reactivity of the cobalt–hydride complex toward a variety of unsaturated substrates is explored to demonstrate its ability to undergo insertion reactions.

## RESULTS AND DISCUSSION

**Synthesis of a Cobalt–Hydride Complex.** Addition of 1 equiv of pyridine-*N*-oxide to **1** results in a red-orange solution and evolution of gaseous N<sub>2</sub> (Scheme 2). The <sup>1</sup>H NMR

Scheme 2



spectrum of the resulting compound (**2**) features 14 paramagnetically shifted resonances, which is indicative of asymmetry in the ligand arrangement. By analogy to the reactions resulting in **1-CO<sub>2</sub>** and **1-Ph<sub>2</sub>CO**,<sup>6d,8</sup> we predicted a Co/Zr  $\mu$ -oxo species, and the solution magnetic moment of **2** was measured to be 3.04  $\mu_B$ , consistent with the same Zr<sup>IV</sup>Co<sup>I</sup>S = 1 configuration adopted by **1-CO<sub>2</sub>** and **1-Ph<sub>2</sub>CO**.

X-ray structure determination of crystals grown from a concentrated pentane solution provided the expected structure of (pyridine)Co(<sup>*i*</sup>Pr<sub>2</sub>PNM<sub>e</sub>)<sub>2</sub>( $\mu$ -O)Zr(<sup>*i*</sup>Pr<sub>2</sub>PNM<sub>e</sub>)<sub>2</sub> (**2**) (Figure 1). To accommodate the bridging oxo ligand, one of the

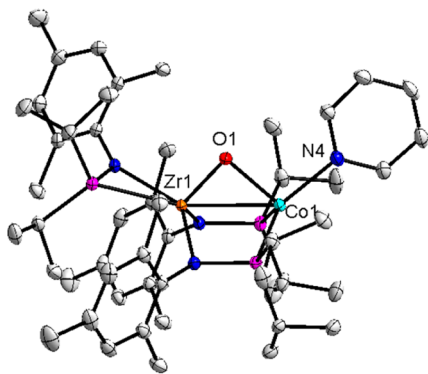


**Figure 1.** Displacement ellipsoid (50%) representation of complex **2**. Hydrogen atoms have been omitted for clarity. Selected interatomic distances (Å) and angles (deg): Zr1–Co1, 2.7086(3); Zr1–O1, 1.8637(11); Co1–O1, 2.0167(11); Co1–N4, 2.0167(11); Zr1–Co1–N4, 141.26(4).

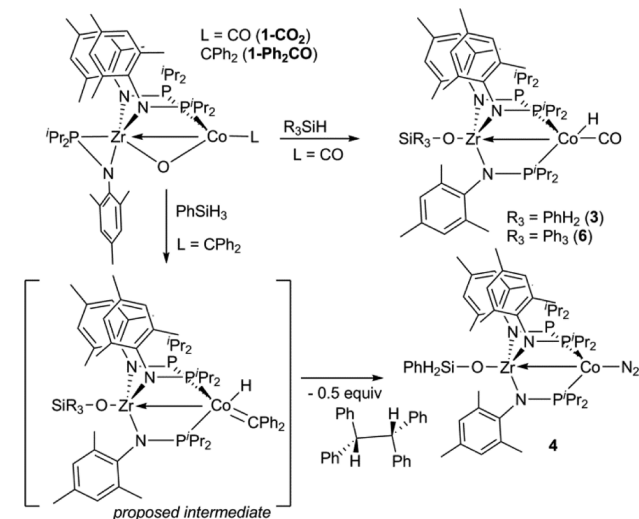
bridging phosphinoamide ligands dissociated from cobalt, resulting in a terminal phosphinoamide ligand-bound  $\eta^2$  to zirconium. Structurally, compound **2** is similar to **1-CO<sub>2</sub>** and **1-Ph<sub>2</sub>CO**,<sup>6d,8</sup> but there are several noteworthy differences. The Zr–Co–L (L = CO, diphenylcarbene, or pyridine) angle of the three  $\mu$ -oxo compounds varies considerably. For L = CO, the Zr–Co–C angle is nearly linear (173.39(11)°), whereas the diphenylcarbene and pyridine ligands are bent much further off the Zr–Co axis (149.24(7) and 141.26(4)°, respectively). While steric considerations likely favor bent Zr–Co–L angles in the pyridine and carbene cases, the position of the strongly  $\pi$  acidic CO ligand in **1-CO<sub>2</sub>** maximizes the orbital overlap for Co–CO  $\pi$  backbonding. The Zr–Co distance in **2** (2.7086(3) Å) is significantly shorter than the Zr–Co distances in **1-CO<sub>2</sub>** or **1-Ph<sub>2</sub>CO** (2.8865(5) and 3.067 Å, respectively), implying that some degree of dative donation from Co to Zr may still be present in complex **2**.

We observed that the formation of both **1-CO<sub>2</sub>** and **1-Ph<sub>2</sub>CO** is impeded by the presence of excess N<sub>2</sub>;<sup>8</sup> however, the formation of **2** proceeded quickly under a N<sub>2</sub> atmosphere, as observed by the rapid evolution of N<sub>2</sub> gas upon addition of pyridine-*N*-oxide to **1**. While N<sub>2</sub> dissociation is necessary for all three reactions to proceed, pyridine-*N*-oxide is a stronger oxidant than CO<sub>2</sub> or benzophenone, and this characteristic may lead to a more facile reaction with **1**.

Complex **2** is unstable at room temperature in solution. Over the course of a week, resonances corresponding to **2** are gradually replaced with the new resonances of an unknown decomposition product in the <sup>1</sup>H NMR spectrum (Supporting Information Figure S13). Due to this instability, we chose to generate **2** in situ for all further studies of its reactivity.

The  $\mu$ -oxo complexes **1-CO<sub>2</sub>** and **1-Ph<sub>2</sub>CO** were both previously shown to react rapidly with 1 equiv of phenylsilane via Si–H bond addition across the Co–O bond to form new terminal Zr–siloxide complexes (Scheme 3).<sup>6d,8</sup> In the case of

Scheme 3

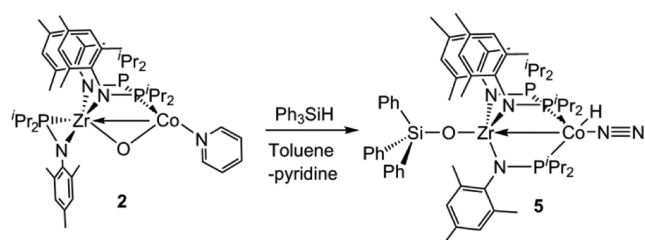


**1-CO<sub>2</sub>**, the Si–H bond of PhSiH<sub>3</sub> adds across the Co–O bond, and the ligands rearrange to afford the cobalt–hydride complex (OC)(H)Co(<sup>*i*</sup>Pr<sub>2</sub>PNM<sub>e</sub>)<sub>3</sub>ZrOSiH<sub>2</sub>Ph (**3**).<sup>6d</sup> Complex **3** is remarkably unreactive, and insertions of unsaturated substrates into the cobalt–hydride bond are precluded by the tightly bound CO ligand. In contrast, it was previously reported that

addition of phenylsilane to **1-Ph<sub>2</sub>CO** results in formation of the Co<sup>0</sup>/Zr<sup>IV</sup> species N<sub>2</sub>Co(<sup>i</sup>Pr<sub>2</sub>PNM<sub>es</sub>)<sub>3</sub>ZrOSiH<sub>2</sub>Ph (**4**) with concomitant extrusion of 0.5 equiv of tetraphenylethane.<sup>8</sup> It was proposed that a cobalt–hydride complex similar to **3** is initially formed en route to **4**, followed by carbene insertion into the cobalt–hydride and homolysis of the Co–C bond in the resulting cobalt(I) alkyl (Scheme 3).

To generate an isolable yet reactive cobalt–hydride species, complex **2** was treated with a silane reagent in a similar fashion. Ph<sub>3</sub>SiH was chosen rather than PhSiH<sub>3</sub> in this case to circumvent any complications arising from remaining Si–H bonds in subsequent reactivity studies (vide infra). When Ph<sub>3</sub>SiH is added to **2** in toluene, the diamagnetic complex (N<sub>2</sub>)(H)Co(<sup>i</sup>Pr<sub>2</sub>PNM<sub>es</sub>)<sub>3</sub>ZrOSiPh<sub>3</sub> (**5**) is produced (Scheme 4). X-ray structure determination of yellow-orange crystals of **5**

Scheme 4



confirmed its connectivity (Figure 2). Compound **5** crystallizes in the rhombohedral crystal class with the molecule lying on a three-fold axis, complicating the location of the hydride electron density. Nonetheless, the cobalt–hydride formulation of **5** is unambiguous because of the broad upfield hydride signal at  $\delta -14.5$  ppm in the <sup>1</sup>H NMR spectrum. A  $\nu(\text{N}_2)$  stretch at 2094 cm<sup>-1</sup> is observed in the solution infrared spectrum of **5**, indicative of a weakly bound dinitrogen ligand. Indeed, a solution of **5** changes color from yellow to red upon removal of the volatiles in vacuo, likely due to the dissociation of the dinitrogen ligand. Performing the reaction of **2** with Ph<sub>3</sub>SiH under argon rather than nitrogen also results in a red solution, but efforts to isolate and structurally characterize a N<sub>2</sub>-free version of **5** were unsuccessful. We hypothesize that a four-coordinate, tetrahedral cobalt–hydride complex is generated upon nitrogen dissociation from **5**. Three- or four-coordinate cobalt–hydride complexes are rare,<sup>13</sup> and in the absence of structural evidence, we cannot rule out a dimeric structure.

In order to probe the origin of the broadening of the hydride signal at  $\delta -14.5$  ppm, the <sup>1</sup>H NMR spectrum of **5** was investigated at low temperature (Supporting Information Figure S3). Upon being cooled to  $-40$  °C, the <sup>1</sup>H NMR spectrum of **5** in deuterated toluene revealed an overlapping doublet of triplets centered at  $\delta -14.5$  ppm with <sup>2</sup>J<sub>H-P</sub> coupling constants of 48 and 68 Hz. This coupling pattern arises from coupling of the hydride proton to two inequivalent types of phosphinoamide phosphorus atoms, in a geometry best described as hydride-capped tetrahedral. A similar multiplet is observed in the upfield region of the <sup>1</sup>H NMR spectrum of the analogous CO-bound cobalt–hydride complex **3** at room temperature.<sup>6d</sup> At room temperature, the <sup>31</sup>P{<sup>1</sup>H} NMR spectrum features two very broad signals at 63.5 and 54.7 ppm in a 2:1 integral ratio. Much like the hydride signal, these two spectral features sharpen and the more upfield signal splits into a doublet at low temperature ( $-60$  °C, Supporting Information Figure S4). Thus, it is likely that lability of the dinitrogen ligand in solution at room temperature is responsible for the broadening of the <sup>31</sup>P NMR signals and the broadening of the hydride signal in the <sup>1</sup>H NMR spectrum of **5**.

The lability of the Co-bound dinitrogen ligand in complex **5** was further demonstrated by its substitution with CO to afford (CO)(H)Co(<sup>i</sup>Pr<sub>2</sub>PNM<sub>es</sub>)<sub>3</sub>ZrOSiPh<sub>3</sub> (**6**), which can alternatively be synthesized via triphenylsilane addition to **1-CO<sub>2</sub>**. The infrared spectrum of compound **6** features a characteristic  $\nu(\text{CO})$  vibration at 1905 cm<sup>-1</sup>, and X-ray crystallography revealed a structure isomorphous to that of **5** (Figure 2). The Co–Zr distance in compound **6** (2.7758(4) Å) is elongated with respect to **5** (2.6977(4) Å) due to the weaker Co→Zr dative interaction that results from stronger  $\pi$  acidity of CO relative to the N<sub>2</sub>. Much like **3**, the hydride signal in the room temperature <sup>1</sup>H NMR spectrum of **6** is a well-defined overlapping doublet of triplets that appears as a quartet at  $\delta -13.9$  ppm (<sup>2</sup>J<sub>H-P</sub> = 21.5 Hz), providing further evidence that the broadening of the analogous signal for **5** is related to the weakly bound N<sub>2</sub> ligand.

**Reactivity of Cobalt–Hydride Complex 5.** Given the lability of the N<sub>2</sub> ligand, we sought to explore the reactivity of the low-coordinate cobalt–hydride compound **5**. Addition of diphenyldiazomethane to compound **5** afforded a new paramagnetic species (Scheme 5). The new compound was structurally characterized and found to be the S = 1 ( $\mu_{\text{eff}} = 3.25 \mu_{\text{B}}$ ) cobalt–hydrazonato complex (Ph<sub>2</sub>C=NNH)Co-

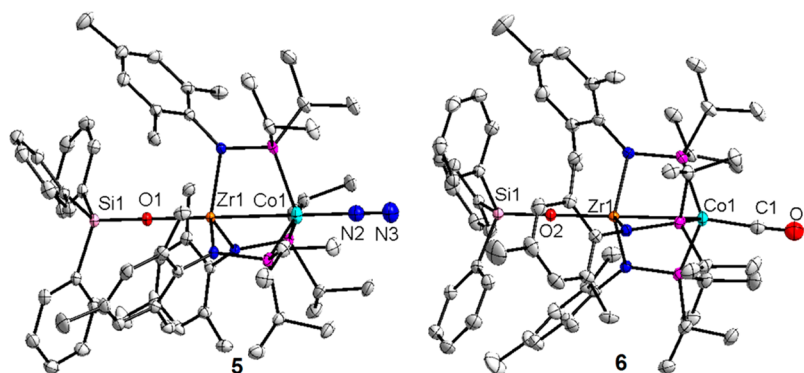
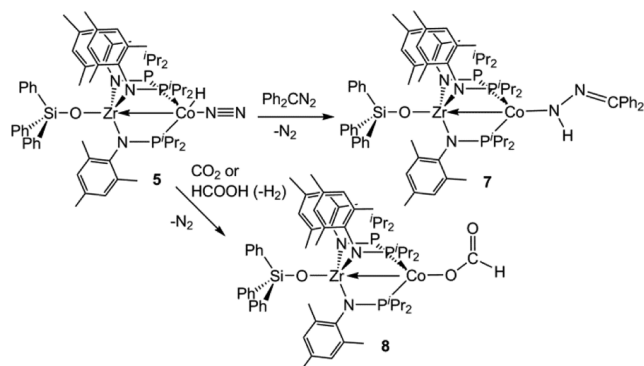


**Figure 2.** Displacement ellipsoid (50%) representation of complexes **5** and **6**. Hydrogen atoms have been omitted for clarity. Selected interatomic distances (Å) and angles (deg): (for **5**) Zr1–Co1, 2.6977(4); Zr1–O1, 1.9856(17); Co1–N2, 1.854(3); (for **6**) Zr1–Co1, 2.7758(4); Zr1–O1, 1.9785(13); Co1–C1, 1.748(3). The Co-bound hydride ligands of compounds **5** and **6** were not located crystallographically.

Scheme 5



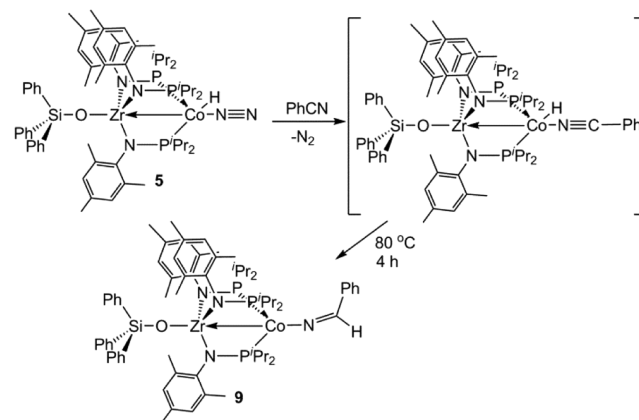
(<sup>i</sup>Pr<sub>2</sub>PNMes)<sub>3</sub>ZrOSiPh<sub>3</sub> (7), resulting from 1,1-insertion of the diazomethane reagent into the cobalt–hydride bond (Figure 3). There are a few reports of migration of a metal–hydride to the  $\alpha$ -N of a bound diazoalkane,<sup>14</sup> with the most well-defined example being the insertion of 9-diazofluorene into the Ru–hydride bond of a (<sup>t</sup>Bu-PNP)Ru<sup>II</sup> dihydride compound (<sup>t</sup>Bu-PNP = 2,6-bis(di-*tert*-butylphosphinomethyl)pyridine).<sup>14c</sup> However, the  $\eta^1$ -hydrazonato complex 7 is a rare example of a structurally characterized compound with this binding mode. For compound 7, the N4–N5 and N5–C64 distances of 1.349(4) and 1.310(5) Å, respectively, are similar to the N–N and N–C distances in Pd(dppf)(*o*-MeC<sub>6</sub>H<sub>4</sub>)(NH–N=CPh<sub>2</sub>) (dppf = 1,1'-bis(diphenylphosphino)ferrocene), (D<sup>t</sup>BPP)Ir(H)(NH–N=CPh<sub>2</sub>) (D<sup>t</sup>BPP = [HC(CH<sub>2</sub>CH<sub>2</sub>P<sup>t</sup>Bu<sub>2</sub>)<sub>2</sub>]<sup>-</sup>), and (PCP)Ir(H)(NH–N=CPh<sub>2</sub>) (PCP = [2,6-(<sup>t</sup>Bu<sub>2</sub>PCH<sub>2</sub>)<sub>2</sub>C<sub>6</sub>H<sub>3</sub>]<sup>-</sup>).<sup>15</sup>

Because cobalt–hydride compounds have recently been reported as active catalysts for the hydrogenation of CO<sub>2</sub> to formate,<sup>9b</sup> the reactivity of hydride compound 5 with CO<sub>2</sub> was explored (Scheme 5). Addition of excess CO<sub>2</sub> to a benzene solution of 5 resulted in immediate formation of blue microcrystals of a new compound. A <sup>1</sup>H NMR spectrum of the blue crystalline compound in CD<sub>2</sub>Cl<sub>2</sub> shows seven paramagnetically shifted peaks, and the solution infrared spectrum features a strong absorption in the region diagnostic for C=O functionalities (1616 cm<sup>-1</sup>). Solution magnetic moment studies by the method of Evans' revealed the product to be  $S = 1$  ( $\mu_{\text{eff}} = 2.86 \mu_{\text{B}}$ ), and X-ray structure determination confirmed its identity as the formate complex (OC(H)O)Co(<sup>i</sup>Pr<sub>2</sub>PNMes)<sub>3</sub>ZrOSiPh<sub>3</sub> (8, Figure 3). Compound 8 crystallizes

in the cubic space group  $P2_13$ , and the location of 8 on a three-fold axis causes considerable disorder of the formate ligand. In order to confirm the identity of compound 8 as a Co<sup>I</sup>–formate, 1 equiv of formic acid was added to compound 5, resulting in the formation of blue microcrystals spectroscopically identical to 8. Similar terminal and bridging iron–formate compounds resulting from the insertion of CO<sub>2</sub> into an iron–hydride bond have been structurally characterized by Holland and Milstein.<sup>16</sup> Moreover, H(N<sub>2</sub>)Co[P(C<sub>6</sub>H<sub>5</sub>)<sub>3</sub>]<sub>3</sub> was also shown to react with CO<sub>2</sub> and formic acid to give the corresponding Co–formate species.<sup>17</sup> Attempts to catalytically reduce CO<sub>2</sub> (1 atm) with 8 using a sacrificial silane reductant were unsuccessful, although CO<sub>2</sub> hydrogenation reactions occur at higher temperatures.

Having demonstrated the ability of compound 5 to undergo insertion reactions with diphenyldiazomethane and CO<sub>2</sub>, we sought to explore the reactivity of 5 with other substrates containing  $\pi$  bonds. Upon addition of benzonitrile to 5, a purple solution containing a diamagnetic product was initially formed, likely a result of substitution of benzonitrile for dinitrogen (Scheme 6 and Supporting Information Figure S9).

Scheme 6



While this intermediate could not be isolated in pure form, an infrared stretch observed at 2161 cm<sup>-1</sup> suggested a Co-bound benzonitrile ligand. Heating the reaction mixture to 80 °C for 4 h results in a color change to red-orange, and paramagnetic compound 9 is formed. Similar to complexes 7 and 8, a solution magnetic moment of 2.95  $\mu_{\text{B}}$  was measured for compound 9, indicative of a molecule with a triplet ground state. X-ray

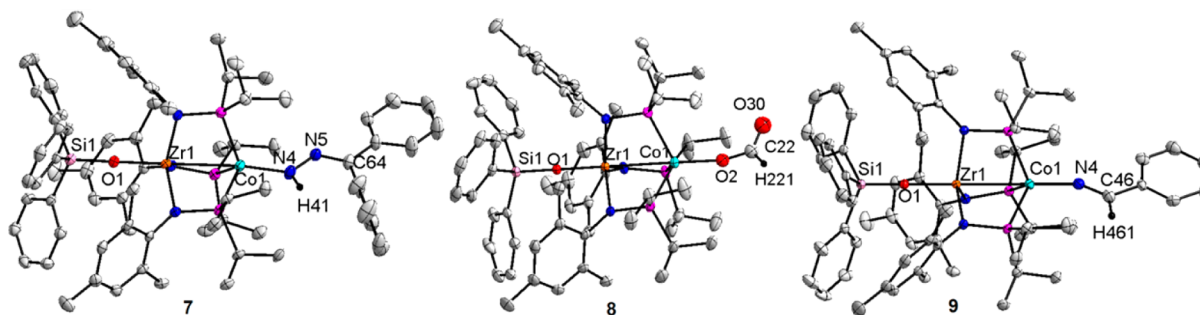


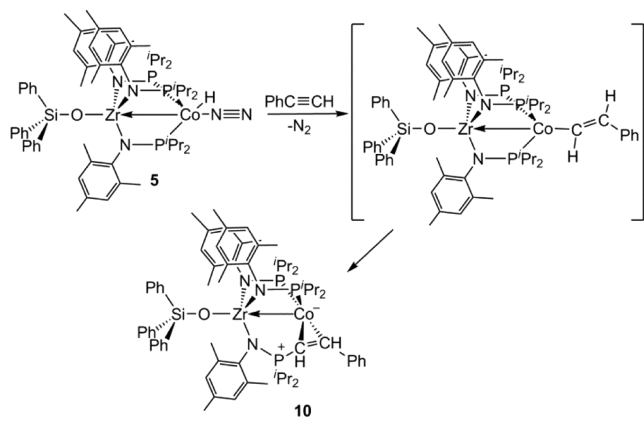
**Figure 3.** Displacement ellipsoid (50%) representation of complexes 7, 8, and 9. Hydrogen atoms except for H41 in 7, H221 in 8, and H461 in 9 have been omitted for clarity. H41 of complex 8 was located in the difference map and refined isotropically. Selected interatomic distances (Å) and angles (deg): (for 7) Zr1–Co1, 2.8250(6); Zr1–O1, 1.978(2); Co1–N4, 1.918(3); Co1–N4, 1.918(3); N4–N5, 1.349(4); N4–H41, 0.81(3); N5–C64, 1.310(5); N4–N5–C64, 120.9(3); (for 8) Zr1–Co1, 2.8141(5); Zr1–O1, 1.964(2); Co1–O2, 1.986(3); (for 9) Zr1–Co1, 2.7914(3); Zr1–O1, 1.9814(13); Co1–N4, 1.8724(17); N4–C46, 1.258(3); Co1–N4–C46, 154.51(16).

structure determination identified the final product as the ketimide compound  $(\text{PhHC}=\text{N})\text{Co}(\text{}^i\text{Pr}_2\text{PNMes})_3\text{ZrOSiPh}_3$  (**9**, Figure 3). The  $\text{N4}-\text{C46}-\text{C47}$  bond angle of  $125.5(2)^\circ$  is indicative of the  $\text{sp}^2$  hybridization of C46 and confirms the assignment of the terminal ligand in **9** as a ketimide.

Formation of the ketimide complex **9** is among several examples of migratory insertion of a nitrile into a metal–hydride bond.<sup>16b,18</sup> Budzelaar and co-workers reported the insertion of an aryl nitrile into a transient cobalt–hydride to form  $(\text{PDI})\text{Co}(\text{N}=\text{CHC}_6\text{H}_4\text{Cl})$  ( $\text{PDI} = (2,6\text{-bis}(2,6\text{-dimethylphenyliminoethyl)pyridine})$ ).<sup>18b</sup> In contrast, the  $\text{Co}-\text{N4}$  bond distance in compound **9** ( $1.8724(17)$  Å) is significantly longer than that in the diamagnetic  $(\text{PDI})\text{CoN}=\text{CHC}_6\text{H}_4\text{Cl}$  ( $1.726(4)$  Å) but is in line with the  $\text{Fe}-\text{N}$  distance in the high-spin  $\beta$ -diketiminato Fe ketimide  $\text{L}^{\text{tBu}}\text{Fe}(\text{N}=\text{CH}^t\text{Bu})$  reported by Holland ( $\text{L}^{\text{tBu}} = [\text{HC}(\text{CMeN}[2,6\text{-diisopropylphenyl}]_2)^-]$ ).<sup>16b</sup> The longer  $\text{Co}-\text{N4}$  distance in **9** relative to that in  $(\text{PDI})\text{Co}(\text{N}=\text{CHC}_6\text{H}_4\text{Cl})$  is consistent with the more bent  $\text{Co}-\text{N4}-\text{C46}$  ( $154.51(16)^\circ$ ) angle in **9**, indicative of negligible  $\pi$  donation from the ketimide nitrogen.

Compound **5** also reacts with phenylacetylene to initially afford a green paramagnetic product that gradually converts to a red diamagnetic compound at room temperature over 24 h (Scheme 7 and Supporting Information Figure S10). The  $^1\text{H}$

Scheme 7



and  $^{31}\text{P}$  NMR spectra of the new red compound **10** are indicative of an asymmetric product with three inequivalent phosphorus environments. Complex **10** can be purified by crystallization to give X-ray quality crystals, and structure determination reveals the final product to be  $\text{Co}(\text{PhHC}=\text{CHP}^i\text{Pr}_2\text{NMes})(\text{}^i\text{Pr}_2\text{PNMes})_2\text{ZrOSiPh}_3$  (**10**, Figure 4). The  $^{31}\text{P}$  NMR spectrum of **10** has three resonances at  $\delta$  63, 47, and 45 ppm, corresponding to the phosphonium phosphorus and two inequivalent phosphine ligands. The green paramagnetic intermediate observed en route to **10** is likely the alkenyl insertion product, namely,  $(\text{PhHC}=\text{CH})\text{Co}(\text{}^i\text{Pr}_2\text{PNMes})_3\text{ZrOSiPh}_3$ , from which compound **10** could form via reductive elimination. Similar  $\text{P}-\text{C}$  reductive elimination reactions from metal phosphine/alkenyl compounds to form the corresponding phosphonium complexes have been documented for Rh and Pd.<sup>19</sup> Unfortunately, a  $\text{C}=\text{C}$  stretch could not be distinguished by IR spectroscopy of the crude reaction mixture of **5** and phenylacetylene to confirm the intermediacy of an alkenyl product.

Unlike the other insertion compounds **7–9**, complex **10** features a short  $\text{Co}-\text{Zr}$  distance of  $2.3738(3)$  Å that is

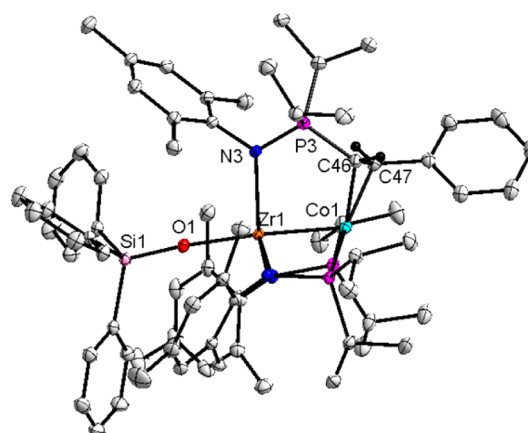


**Figure 4.** Displacement ellipsoid (50%) representation of complex **10**. Hydrogen atoms except for those bound to C46 and C47 have been omitted for clarity. Selected interatomic distances (Å) and angles (deg):  $\text{Zr1}-\text{Co1}$ ,  $2.3738(3)$ ;  $\text{Zr1}-\text{O1}$ ,  $2.0573(11)$ ;  $\text{Co1}-\text{C46}$ ,  $1.9654(16)$ ;  $\text{Co1}-\text{C47}$ ,  $1.9844(16)$ ;  $\text{C46}-\text{C47}$ ,  $1.458(2)$ ;  $\text{P3}-\text{C46}$ ,  $1.7652(16)$ .

comparable to that of **1** ( $2.33(1)$  Å).<sup>6b</sup> This observed increase in  $\text{Co}-\text{Zr}$  bond order likely occurs due to the more electron-rich  $\text{Co}^{-1}$  datively donating electron density to zirconium. The contracted  $\text{Co}-\text{Zr}$  distance is accompanied by a  $\sim 0.1$  Å elongation of the  $\text{Zr}-\text{O}$  bond distance ( $2.0573(11)$  Å) compared to compounds **7–9**, as would be expected due to a *trans*-influence from the  $\text{Co}\rightarrow\text{Zr}$  bond.

In contrast to phenylacetylene, insertion products are not isolated when **5** is treated with olefins. When stoichiometric 1-hexene was added to compound **5**, no new  $\text{Co}/\text{Zr}$  compounds were observed by  $^1\text{H}$  and  $^{31}\text{P}$  NMR spectroscopy; however, 1-hexene was isomerized to internal hexene isomers. Compound **5** was found to be an active catalyst for 1-hexene isomerization, and complete conversion of 1-hexene to 98% *cis/trans* 2-hexene occurred within 30 h at  $65^\circ\text{C}$  using 1 mol % of compound **5** (Supporting Information Figure S12). The mechanism of this reaction is unknown at this time; however, a recent report has demonstrated *Z*-selective olefin isomerization using a cobalt alkyl catalyst,<sup>20</sup> so a cobalt alkyl intermediate may be plausible. Selective olefin isomerization reactions are important with respect to several organometallic catalytic transformations, including olefin oligomerizations and olefin metathesis;<sup>21</sup> however, olefin isomerizations to yield terminal olefins rather than internal olefins would be more economically desirable.

## CONCLUSION

In summary, pyridine-*N*-oxide reacts with the reduced  $\text{Co}/\text{Zr}$  heterobimetallic complex **1** via a two-electron oxidation in a manner analogous to its reactivity with  $\text{CO}_2$  and ketones. The flexibility of the tris(phosphinoamide) ligand framework allows reversible metal–metal bond formation/cleavage upon redox events and allows substrates to access both metal centers by reversible dissociation of the phosphine donor ligand from  $\text{Co}$ . Addition of  $\text{Ph}_3\text{SiH}$  to the pyridine-*N*-oxide product **2** generates a  $\text{Co}^{\text{I}}-\text{hydride}$  complex **5** in which the  $\text{C}_3$ -symmetric tris(phosphinoamide) ligand framework has been restored.

The coordination environment of cobalt in the  $\text{Co}^{\text{I}}(\text{N}_2)\text{H}$  complex **5** is, on the surface, quite similar to that of the  $\text{H}(\text{N}_2)\text{Co}[\text{P}(\text{C}_6\text{H}_5)_3]_3$  complex reported by Ibers et al.,<sup>22</sup> but the tripodal ligand framework in **5** enforces a *cis*-configuration of the hydride and  $\text{N}_2$  ligands. Complex **5** is highly reactive,

which is in stark contrast to the analogous  $\text{Co}^{\text{I}}(\text{CO})\text{H}$  complexes **3** and **6**. The lability of the dinitrogen ligand allows complex **5** to exhibit reactivity that might be expected for a four-coordinate metal–hydride. Insertion of unsaturated substrates into the cobalt–hydride bond leads to a series of compounds featuring unusual binding modes, including an  $\eta^1$ -hydrazonato, a terminal formate, and an  $\eta^1$ -ketimide complex. Since such reactivity is not observed for the CO-bound analogues **3** and **6**, it can be concluded that  $\text{N}_2$  dissociation to form a four-coordinate cobalt–hydride intermediate is a necessary requisite for these reactions to proceed.

Although the heterobimetallic nature of complex **5** does not appear to play a significant role in its reactivity, reversible metal–metal bond formation/cleavage does play an important role in the formation of this reactive compound via heterolytic Si–H bond cleavage.

## EXPERIMENTAL SECTION

**General Considerations.** All manipulations were carried out under an inert atmosphere using a nitrogen-filled glovebox or standard Schlenk techniques unless otherwise noted. All glassware was oven- or flame-dried immediately prior to use. Diethyl ether was obtained as high-performance liquid chromatography grade without inhibitors; pentane and benzene were obtained as ACS reagent grade. All protio solvents were degassed by sparging with ultra-high-purity argon and dried via passage through columns of drying agents using a Seca solvent purification system from Pure Process Technologies. Benzene- $d_6$  was degassed and dried over 4 Å molecular sieves before use. THF- $d_8$  and  $\text{CD}_2\text{Cl}_2$  were dried over  $\text{CaH}_2$ , vacuum-transferred, and degassed via repeated freeze–pump–thaw cycles. For  $^1\text{H}$  and  $^{13}\text{C}\{^1\text{H}\}$  NMR spectra, the solvent resonance was referenced as an internal standard. For  $^{31}\text{P}\{^1\text{H}\}$  NMR spectra, 85%  $\text{H}_3\text{PO}_4$  was used as an external standard (0 ppm). For the paramagnetic molecules (**2**, **7**, **8**, and **9**), the  $^1\text{H}$  NMR data are reported with the chemical shift, followed by the peak width at half height, integration, and tentative assignment, where possible, in parentheses. Carbon dioxide (bone dry grade 3.0) and carbon monoxide (CP grade 2.5) were purchased from Airgas and used without further purification. Complexes **1**,<sup>6b</sup> **1-CO**,<sup>6a</sup> **1-Ph<sub>2</sub>CO**,<sup>8</sup> **3**,<sup>6d</sup> **4**,<sup>8</sup> and diphenyldiazomethane<sup>23</sup> were synthesized according to literature procedures. All other reagents and solvents were obtained from commercial sources and used without further purification. Infrared spectra were recorded on a Varian 640-IR spectrometer controlled by Resolutions Pro software. UV–vis spectra were recorded on a Cary 50 UV–vis spectrophotometer using Cary WinUV software. Elemental microanalyses were performed by Complete Analysis Laboratories, Inc., Parsippany, NJ. Solution magnetic moments were measured using Evans' method and are reported without taking into account any diamagnetic contributions (Pascal's constants were not used).<sup>24</sup>

**X-ray Crystallography.** All operations were performed on a Bruker-Nonius Kappa Apex2 diffractometer, using graphite-monochromated Mo  $K\alpha$  radiation. All diffractometer manipulations, including data collection, integration, scaling, and absorption corrections, were carried out using the Bruker Apex 2 software.<sup>25</sup> Preliminary cell constants were obtained from three sets of 12 frames. Fully labeled diagrams and data collection and refinement details are included in Tables S1–S3 and on pages S12–S30 of the Supporting Information.

**(Pyridine)Co(<sup>i</sup>Pr<sub>2</sub>PNMes)<sub>2</sub>( $\mu$ -O)Zr(<sup>i</sup>Pr<sub>2</sub>PNMes) (**2**).** A solution containing 0.4334 g (0.4329 mmol) of **1** in toluene (5 mL) was cooled to near freezing. A separate solution of 0.0424 g (0.446 mmol) of pyridine-*N*-oxide in toluene (5 mL) was prepared. The solution containing pyridine-*N*-oxide was added dropwise to the thawing solution containing **1**. The resulting solution changed from a brick-red color to red-orange, and evolution of gas ( $\text{N}_2$ ) was observed during the addition. After being stirred for 20 min, the reaction mixture was filtered and the volatiles were removed from the filtrate in vacuo. Pentane (5 mL) was added to the red solids and concentrated. The red

crystalline product was isolated (0.2954 g, 68%) by decanting the pentane mother liquor. Red X-ray quality crystals were grown from a concentrated pentane solution at  $-35$  °C.  $^1\text{H}$  NMR (400 MHz,  $\text{C}_6\text{D}_6$ ):  $\delta$  20.7 (88 Hz), 10.8 (199 Hz), 7.9 (17 Hz), 7.7 (179 Hz), 6.3 (16 Hz), 6.0 (15 Hz), 5.2 (61 Hz), 2.4 (12 Hz), 1.5 (25 Hz), 0.7 (34 Hz), 0.4 (22 Hz),  $-0.6$  (80 Hz),  $-12.2$  (298 Hz),  $-18.3$  (91 Hz). Note: due to the large number of broad peaks over a wide spectral width, the spectrum could not be reliably assigned or integrated. UV–vis ( $\text{C}_6\text{H}_6$ ,  $\lambda$  (nm)) ( $\epsilon$ ,  $\text{M}^{-1} \text{cm}^{-1}$ ): 465 (720), 675 (160), 829 (110). Evans' method ( $\mu_{\text{eff}}$ ,  $\text{C}_6\text{D}_6$ ): 3.04  $\mu_{\text{B}}$ . Satisfactory elemental analysis data could not be obtained because of the thermal instability of complex **2**.

**(N<sub>2</sub>)(H)Co(<sup>i</sup>Pr<sub>2</sub>PNMes)<sub>3</sub>ZrOSiPh<sub>3</sub> (**5**).** A solution containing 0.5770 g (0.5763 mmol) of **1** in toluene (4 mL) was cooled to near freezing. A separate solution of 0.0565 g (0.594 mmol) of pyridine-*N*-oxide (py-O) in toluene (4 mL) was prepared. The solution containing py-O was added dropwise to the thawing solution containing **1**. The resulting solution changed from a brick-red color to red-orange, and evolution of gas ( $\text{N}_2$ ) was observed during the addition. After being stirred for 20 min, a solution of 0.1551 g of  $\text{Ph}_3\text{SiH}$  (0.5956 mmol) in toluene (2 mL) was added dropwise to the stirring reaction mixture. The reaction was allowed to stir for 20 min, and the reaction mixture was filtered. The volatiles were removed from the filtrate in vacuo. The remaining yellow-brown solids were washed with cold pentane (5 mL), leaving the analytically pure product (0.4436 g, 64%). Yellow X-ray quality crystals were grown via vapor diffusion of pentane into a concentrated benzene solution of **5** at room temperature.  $^1\text{H}$  NMR (400 MHz,  $\text{C}_6\text{D}_6$ ):  $\delta$  7.26 (t, 3H,  $^3J_{\text{HH}} = 7.6$  Hz, Si–Ar), 7.07 (t, 6H,  $^3J_{\text{HH}} = 7.6$  Hz, Si–Ar), 6.71 (s, 6H, Mes), 6.39 (d, 6H,  $^3J_{\text{HH}} = 6.8$  Hz, Si–Ar), 2.84 (br m, 6H,  $\text{CH}(\text{CH}_3)_2$ ), 2.23 (s, 9H, Mes-Me), 2.16 (s, 18H, Mes-Me), 1.54 (br d, 18H,  $^3J_{\text{HH}} = 5.2$ ,  $\text{CH}(\text{CH}_3)_2$ ), 1.35 (br d, 18H,  $^3J_{\text{HH}} = 6$  Hz,  $\text{CH}(\text{CH}_3)_2$ ),  $-14.47$  (br, 1H,  $^2J_{\text{HP}} = 68$  Hz and  $^2J_{\text{HP}} = 48$  Hz (coupling constants from  $-40$  °C collection), Co–H).  $^{31}\text{P}\{^1\text{H}\}$  NMR (161.8 MHz,  $\text{C}_6\text{D}_6$ ):  $\delta$  63.5 (v br, 1P), 54.7 (v br, 2P).  $^{13}\text{C}\{^1\text{H}\}$  NMR (100.5 MHz,  $\text{C}_6\text{D}_6$ ):  $\delta$  148.2 (*ipso*-Mes), 137.1 (Si–Ar), 136.6 (Mes), 134.7 (Si–Ar), 132.4 (Mes), 129.7 (Si–Ar), 129.1 (Mes), 127.1 (Si–Ar), 42.7 (v br,  $\text{PC}(\text{CH}_3)_2$ ), 23.1 ( $\text{PC}(\text{CH}_3)_2$ ), 22.7 (Mes-Me), 22.6 ( $\text{PC}(\text{CH}_3)_2$ ), 20.8 (Mes-Me). IR ( $\text{C}_6\text{H}_6$ ): 2094  $\text{cm}^{-1}$  ( $\nu_{\text{N}}$ ). UV–vis ( $\text{C}_6\text{H}_6$ ,  $\lambda$  (nm)) ( $\epsilon$ ,  $\text{M}^{-1} \text{cm}^{-1}$ ): 505 (440), 612 (210). Anal. Calcd for  $\text{C}_66\text{H}_{91}\text{N}_5\text{O}_3\text{ZrCoSi}$ : C, 62.76; H, 7.61; N, 5.81. Found: C, 62.67; H, 7.59; N, 5.77.

**(OC)(H)Co(<sup>i</sup>Pr<sub>2</sub>PNMes)<sub>3</sub>ZrOSiPh<sub>3</sub> (**6**).** Two solutions, one containing 0.1040 g (0.1100 mmol) of **1-CO**<sub>2</sub> in toluene (2 mL) and another containing 0.0287 g (0.110 mmol) of triphenylsilane in toluene (2 mL), were cooled to near freezing. The thawing solution containing triphenylsilane was added dropwise to the cold solution containing **1-CO**<sub>2</sub>. After being stirred for 20 min, the volatiles were removed in vacuo. The remaining yellow solids were washed with pentane and extracted into toluene. After filtration, the volatiles were removed from the filtrate in vacuo to yield analytically pure product (0.101 g, 76%) as a yellow solid. Yellow prismatic crystals, sufficient for X-ray diffraction, were grown at room temperature from a concentrated diethyl ether solution of **6**.  $^1\text{H}$  NMR (400 MHz,  $\text{C}_6\text{D}_6$ ):  $\delta$  7.28 (t, 3H,  $^3J_{\text{HH}} = 6.8$  Hz, Si–Ar), 7.08 (t, 6H,  $^3J_{\text{HH}} = 7.2$  Hz, Si–Ar), 6.69 (s, 6H, Mes), 6.39 (d, 6H,  $^3J_{\text{HH}} = 6.4$  Hz, Si–Ar), 2.63 (br m, 6H,  $\text{CH}(\text{CH}_3)_2$ ), 2.22 (s, 9H, Mes-Me), 2.13 (s, 18H, Mes-Me), 1.64 (br, 18H,  $\text{CH}(\text{CH}_3)_2$ ), 1.32 (br, 18H,  $\text{CH}(\text{CH}_3)_2$ ),  $-13.93$  (apt q, 1H,  $^2J_{\text{PH}} = 21.5$  Hz and  $^2J_{\text{PH}} = 21.5$  Hz, Co–H).  $^{31}\text{P}\{^1\text{H}\}$  NMR (161.8 MHz,  $\text{C}_6\text{D}_6$ ):  $\delta$  69.9 (s).  $^{13}\text{C}\{^1\text{H}\}$  NMR (100.5 MHz,  $\text{C}_6\text{D}_6$ ):  $\delta$  148.3 (*ipso*-Mes), 137.1 (Si–Ar), 136.1 (Mes), 134.6 (Si–Ar), 132.6 (Mes), 129.8 (Si–Ar), 129.3 (Mes), 127.2 (Si–Ar), 43.0 ( $\text{PC}(\text{CH}_3)_2$ ), 23.7 ( $\text{PC}(\text{CH}_3)_2$ ), 22.6 (Mes-Me), 22.5 ( $\text{PC}(\text{CH}_3)_2$ ), 20.8 (Mes-Me). IR ( $\text{C}_6\text{H}_6$ ): 1905  $\text{cm}^{-1}$  ( $\nu_{\text{CO}}$ ). UV–vis ( $\text{C}_6\text{H}_6$ ,  $\lambda$  (nm)) ( $\epsilon$ ,  $\text{M}^{-1} \text{cm}^{-1}$ ): 362 (2900), 511 (100). Anal. Calcd for  $\text{C}_{64}\text{H}_{91}\text{N}_5\text{O}_2\text{P}_3\text{ZrCoSi}$ : C, 63.76; H, 7.61; N, 3.49. Found: C, 63.87; H, 7.79; N, 3.52.

**(Ph<sub>2</sub>CN=NH)Co(<sup>i</sup>Pr<sub>2</sub>PNMes)<sub>3</sub>ZrOSiPh<sub>3</sub> (**7**).** Two solutions, one containing 0.0305 g (0.0253 mmol) of **5** in toluene (2 mL) and another containing 0.0052 g (0.027 mmol) of diphenyldiazomethane in toluene (2 mL), were cooled to near freezing. The thawing solution

containing diphenyldiazomethane was added dropwise to the cold solution containing **5**. The reaction mixture was allowed to stir for 1 h. The volatiles were removed in vacuo. The remaining solid was washed with cold pentane to yield an analytically pure green-brown solid (0.0202 g, 58%). X-ray quality crystals were grown from concentrated pentane at room temperature over 24 h.  $^1\text{H}$  NMR (400 MHz,  $\text{C}_6\text{D}_6$ ):  $\delta$  22.6 (79 Hz, 2H,  $\text{Ph}_2\text{CN}=\text{NH}$ ), 16.0 (273 Hz, 18H,  $^i\text{PrMe}$ ), 14.1 (81 Hz, 2H,  $\text{Ph}_2\text{CN}=\text{NH}$ ), 7.5 (18 Hz, 3H,  $\text{Ph}_3\text{Si}$ ), 6.8 (44 Hz, 12H, 2 overlapping  $\text{Ph}_3\text{Si}$  or Mes-Ar peaks), 6.4 (32 Hz, 6H,  $\text{Ph}_3\text{Si}$  or Mes-Ar), 4.2 (42 Hz, 2H,  $\text{Ph}_2\text{CN}=\text{NH}$ ), 1.9 (19 Hz, 27H, MesMe +  $^i\text{PrMe}$ ), -1.1 (v br, 18H, MesMe), -34.9 (140 Hz, 2H,  $\text{Ph}_2\text{CN}=\text{NH}$ ), -39.9 (279 Hz, 2H,  $\text{Ph}_2\text{CN}=\text{NH}$ ). Note: isopropyl methine and  $\text{Ph}_2\text{CN}=\text{NH}$  resonances are not observed. UV-vis ( $\text{C}_6\text{H}_6$ ,  $\lambda$  (nm)) ( $\epsilon$ ,  $\text{M}^{-1} \text{cm}^{-1}$ ): 446 (25000), 582 (1600), 804 (1100). Evans' method ( $\mu_{\text{eff}}$ ,  $\text{C}_6\text{D}_6$ ): 3.25  $\mu_{\text{B}}$ . Anal. Calcd for  $\text{C}_7\text{H}_{10}\text{N}_3\text{OSiP}_3\text{CoZr}$ : C, 66.54; H, 7.42; N, 5.10. Found: C, 66.42; H, 7.23; N, 5.06.

**(OC(H)O)Co( $^i\text{Pr}_2\text{PNMes}_3\text{ZrOSiPh}_3$ ) (8).** A solution containing 0.100 g (0.0830 mmol) of **5** in benzene (5 mL) was placed in a Schlenk tube equipped with a stir bar and sealed with a Teflon valve. The solution was frozen, and the headspace of the flask was evacuated and backfilled with 10 equiv of  $\text{CO}_2$  using a known volume gas bulb and partial pressure methods. The Schlenk tube was sealed, and the solution was allowed to thaw. Immediately upon thawing, blue microcrystals of the product formed and the solution color changed from yellow to pale purple in color. The blue microcrystals were isolated from the benzene solution, extracted into  $\text{CH}_2\text{Cl}_2$ , and dried in vacuo (0.0403 g). The remaining benzene solution can be layered with pentane to isolate additional **8** as a blue solid (0.0312 g). The total combined yield was 0.0715 g, 71%.  $^1\text{H}$  NMR (400 MHz,  $\text{CD}_2\text{Cl}_2$ ):  $\delta$  18.9 (287 Hz, 18H,  $^i\text{Pr-Me}$ ), 7.5 (17 Hz, 3H,  $\text{Ph}_3\text{Si}$ ), 7.1 (20 Hz, 6H,  $\text{Ph}_3\text{Si}$  or Mes-Ar), 6.4 (44 Hz, 6H,  $\text{Ph}_3\text{Si}$  or Mes-Ar), 6.1 (34 Hz, 6H,  $\text{Ph}_3\text{Si}$  or Mes-Ar), 2.0 (13 Hz, 9H, Mes-Me), 1.6 (375 Hz, 18H,  $^i\text{Pr-Me}$ ), -2.0 (v br, 18H, Mes-Me). Note: isopropyl methine and -OCOH resonances are not observed. IR ( $\text{CD}_2\text{Cl}_2$ ): 1616  $\text{cm}^{-1}$  ( $\nu_{\text{C}=\text{O}}$ ). UV-vis ( $\text{CH}_2\text{Cl}_2$ ,  $\lambda$  (nm)) ( $\epsilon$ ,  $\text{M}^{-1} \text{cm}^{-1}$ ): 338 (3800), 578 (77), 868 (190). Evans' method ( $\mu_{\text{eff}}$ ,  $\text{CD}_2\text{Cl}_2$ ): 2.86  $\mu_{\text{B}}$ . Anal. Calcd for  $\text{C}_{64}\text{H}_{91}\text{N}_3\text{O}_3\text{SiP}_3\text{CoZr}$ : C, 62.93; H, 7.51; N, 3.44. Found: C, 62.81; H, 7.41; N, 3.56.

**(PhHC=N)Co( $^i\text{Pr}_2\text{PNMes}_3\text{ZrOSiPh}_3$ ) (9).** Two solutions, one containing 0.0507 g (0.0421 mmol) of **5** in toluene (2 mL) and another containing 4.4  $\mu\text{L}$  (0.043 mmol) of benzonitrile in toluene (2 mL), were cooled to near freezing. The thawing solution containing benzonitrile was added dropwise to the cold solution containing **5**, resulting in a color change from yellow to dark purple. The reaction mixture was stirred and heated at 80  $^\circ\text{C}$  for 4 h, during which the color turned from purple to red-orange. The reaction mixture was concentrated in vacuo and layered with pentane. After 24 h at room temperature, red solids were isolated from the mother liquor and dried in vacuo to afford analytically pure **9** (0.0391 g, 72%). Red X-ray quality crystals were grown from a concentrated toluene solution at room temperature.  $^1\text{H}$  NMR (400 MHz,  $\text{C}_6\text{D}_6$ ):  $\delta$  25.1 (39 Hz, 2H,  $\text{PhHC}=\text{N}$ ), 14.0 (78 Hz, 18H,  $^i\text{Pr-Me}$ ), 7.5 (17 Hz, 3H,  $\text{Ph}_3\text{Si}$ ), 7.2 (6 Hz, 6H,  $\text{Ph}_3\text{Si}$  or Mes-Ar), 6.9 (21 Hz, 6H,  $\text{Ph}_3\text{Si}$  or Mes-Ar), 6.7 (12 Hz, 6H,  $\text{Ph}_3\text{Si}$  or Mes-Ar), 6.4 (14 Hz, 2H,  $\text{PhHC}=\text{N}$ ), 1.9 (8 Hz, 27H, Mes-Me +  $^i\text{PrMe}$ ), -1.0 (219 Hz, 18H, Mes-Me), -11.6 (28 Hz, 1H,  $\text{PhHC}=\text{N}$ ), -16.2 (88 Hz, 1H,  $\text{PhHC}=\text{N}$ ). Note: isopropyl methine resonances are not observed. UV-vis ( $\text{C}_6\text{H}_6$ ,  $\lambda$  (nm)) ( $\epsilon$ ,  $\text{M}^{-1} \text{cm}^{-1}$ ): 343 (9200), 442 (2400), 510 (980), 716 (770). Evans' method ( $\mu_{\text{eff}}$ ,  $\text{C}_6\text{D}_6$ ): 2.95  $\mu_{\text{B}}$ . Anal. Calcd for  $\text{C}_{70}\text{H}_{96}\text{N}_4\text{OSiP}_3\text{CoZr}$ : C, 65.65; H, 7.56; N, 4.37. Found: C, 65.43; H, 7.69; N, 4.24.

**Co(PhHC=CHP $^i\text{Pr}_2\text{NMes}$ )( $^i\text{Pr}_2\text{PNMes}_2\text{ZrOSiPh}_3$ ) (10).** A solution containing 9.5  $\mu\text{L}$  (0.087 mmol) of phenylacetylene in toluene (2 mL) was added dropwise to a stirring solution containing 0.1030 g (0.08543 mmol) of **5** in toluene (3 mL) in a scintillation vial. The reaction mixture initially changed color from yellow to green and was allowed to stir for 24 h until the reaction mixture appeared red in color. The reaction mixture was filtered through a pad of Celite, and the filtrate was concentrated in vacuo. Pentane was layered onto the concentrated toluene solution, and after 24 h, the red-brown product was isolated as an analytically pure solid by decanting the mother

liquor and drying the remaining solids in vacuo (0.0593 g, 54%). Red X-ray quality crystals were grown at room temperature from a concentrated toluene solution layered with pentane.  $^1\text{H}$  NMR (400 MHz,  $\text{C}_6\text{D}_6$ ):  $\delta$  7.29–7.16 (m, ~4H), 7.16–7.01 (m, ~10H), 6.89 (t, 1H,  $^3J_{\text{HH}} = 7.2$  Hz, Ar), 6.74 (d, 2H,  $^3J_{\text{HH}} = 7.2$  Hz, Ar), 6.57 (s, 1H, Mes), 6.48 (s, 1H, Mes), 6.42 (d, 3H,  $^3J_{\text{HH}} = 7.2$  Hz, Si-Ar and Mes), 6.32 (d, 3H,  $^3J_{\text{HH}} = 7.2$  Hz, Si-Ar and Mes), 6.24 (d, 3H,  $^3J_{\text{HH}} = 7.2$  Hz, Si-Ar and Mes), 6.13 (s, 1H, Mes), 3.46 (br m, 1H,  $\text{PC}(\text{H})\text{C}(\text{H})\text{Ph}$ ), 3.16 (m, 2H,  $\text{CH}(\text{CH}_3)_2$ ), 2.99 (m, 4H,  $\text{CH}(\text{CH}_3)_2$ ), 2.74 (s, 3H, Mes-Me), 2.60 (s, 3H, Mes-Me), 2.57 (s, 3H, Mes-Me), 2.47 (br m, 1H,  $\text{PC}(\text{H})\text{C}(\text{H})\text{Ph}$ ), 2.34 (s, 3H, Mes-Me), 2.25 (s, 3H, Mes-Me), 2.22 (s, 3H, Mes-Me), 2.09 (s, 3H, Mes-Me), 1.76 (s, 3H, Mes-Me), 1.61 (m overlap with s, 9H + 3H,  $\text{CH}(\text{CH}_3)_2$  + Mes-Me), 1.34 (m, 15H,  $\text{CH}(\text{CH}_3)_2$ ), 1.04 (m, 6H,  $\text{CH}(\text{CH}_3)_2$ ), 0.83 (dd, 3H,  $^3J_{\text{HH}} = 7.2$  Hz and  $^3J_{\text{HP}} = 15.6$  Hz,  $\text{CH}(\text{CH}_3)_2$ ), 0.66 (m, 3H,  $^3J_{\text{HH}} = 7.2$  Hz and  $^3J_{\text{HP}} = 11.6$  Hz,  $\text{CH}(\text{CH}_3)_2$ ).  $^{31}\text{P}\{^1\text{H}\}$  NMR (161.8 MHz,  $\text{C}_6\text{D}_6$ ):  $\delta$  62.7 (br s, 1P), 47.3 (br s, 1P), 45.9 (br s, 1P).  $^{13}\text{C}\{^1\text{H}\}$  NMR (100.5 MHz,  $\text{C}_6\text{D}_6$ ):  $\delta$  154.1, 150.4, 150.2, 149.1, 149.0, 144.2, 144.1, 139.9, 138.5, 138.0, 137.3, 137.0, 136.6, 135.8, 135.5, 133.6, 133.3, 132.8, 131.2, 130.8, 130.0, 129.2, 129.0, 127.1, 126.7, 126.6, 126.3, 41.7 (m), 40.3, 40.2, 37.4, 35.7, 35.0, 35.2, 35.0, 34.6, 25.9, 25.7, 24.4, 24.0, 23.9, 23.8, 22.9, 22.8, 22.7, 22.3, 21.8, 21.7, 21.6, 21.5, 21.3, 21.1, 21.0, 21.0, 20.9, 20.8, 20.5, 20.4, 18.7, 17.3. UV-vis ( $\text{C}_6\text{H}_6$ ,  $\lambda$  (nm)) ( $\epsilon$ ,  $\text{M}^{-1} \text{cm}^{-1}$ ): 416 (4200). Anal. Calcd for  $\text{C}_{71}\text{H}_{96}\text{N}_3\text{OSiP}_3\text{CoZr}$ : C, 66.69; H, 7.57; N, 3.29. Found: C, 66.57; H, 7.58; N, 3.13.

**1-Hexene Isomerization.** A  $\text{C}_6\text{D}_6$  solution was prepared containing 0.0060 g (0.0050 mmol) of compound **5** and 63  $\mu\text{L}$  (0.50 mmol) of 1-hexene. The  $\text{C}_6\text{D}_6$  reaction mixture was added to a J-Young fitted NMR tube and was heated at 65  $^\circ\text{C}$  for 30 h. The reaction mixture volatiles were vacuum-transferred to a second J-Young fitted NMR tube. The integration of the  $^1\text{H}$  NMR spectrum of the volatile products from the reaction mixture revealed a composition of ~98% *cis/trans* 2-hexene.

## ■ ASSOCIATED CONTENT

### Supporting Information

X-ray data collection, solution, and refinement details for **2** and **5–10**, crystallographic data in CIF format,  $^1\text{H}$  NMR spectra for complexes **2** and **5–10**, variable-temperature  $^1\text{H}$  and  $^{31}\text{P}$  NMR spectra for complex **5**,  $^1\text{H}$  NMR data showing intermediates formed in the reactions of benzonitrile and phenylacetylene with **5**, and  $^1\text{H}$  NMR spectrum of 1-hexene isomerization products. The Supporting Information is available free of charge on the ACS Publications website at DOI: 10.1021/acs.organomet.5b00182.

## ■ AUTHOR INFORMATION

### Corresponding Author

\*E-mail: thomasc@brandeis.edu.

### Notes

The authors declare no competing financial interest.

## ■ ACKNOWLEDGMENTS

We acknowledge financial support from the U.S. Department of Energy under Award DE-SC0004019.

## ■ REFERENCES

- (1) (a) Cotton, F. A.; Murillo, C. A.; Walton, R. A. *Multiple Bonds between Metal Atoms*; Springer Science and Business Media, Inc.: New York, 2005. (b) (Krogman, J. P.; Thomas, C. M. *Chem. Commun.* **2014**, 50, 5115–5127.
- (2) (a) Wheatley, N.; Kalck, P. *Chem. Rev.* **1999**, 99, 3379–3420. (b) Gade, L. H. *Angew. Chem., Int. Ed.* **2000**, 39, 2658–2678. (c) Bullock, R. M.; Casey, C. P. *Acc. Chem. Res.* **1987**, 20, 167–173. (d) Stephan, D. W. *Coord. Chem. Rev.* **1989**, 95, 41–107. (e) Cooper,

- B. G.; Napoline, J. W.; Thomas, C. M. *Catal. Rev.: Sci. Eng.* **2012**, *54*, 1–40.
- (3) Tauster, S. J.; Fung, S. C.; Garten, R. L. *J. Am. Chem. Soc.* **1978**, *100*, 170–175.
- (4) (a) Bradford, M. C. J.; Vannice, M. A. *J. Catal.* **1998**, *173*, 157–171. (b) Bitter, J. H.; Seshan, K.; Lercher, J. A. *J. Catal.* **1997**, *171*, 279–286. (c) Tauster, S. J. *Acc. Chem. Res.* **1987**, *20*, 389–394.
- (5) (a) Bernal, S.; Calvino, J. J.; Cauqui, M. A.; Gatica, J. M.; López Cartes, C.; Pérez Omil, J. A.; Pintado, J. M. *Catal. Today* **2003**, *77*, 385–406. (b) Bernal, S.; Calvino, J. J.; Cauqui, M. A.; Gatica, J. M.; Lares, C.; Pérez Omil, J. A.; Pintado, J. M. *Catal. Today* **1999**, *50*, 175–206. (c) Huizinga, T.; Prins, R. *J. Phys. Chem.* **1981**, *85*, 2156–2158. (d) Sadeghi, H. R.; Henrich, V. E. *J. Catal.* **1988**, *109*, 1–11. (e) Sakellson, S.; McMillan, M.; Haller, G. L. *J. Phys. Chem.* **1986**, *90*, 1733–1736.
- (6) (a) Thomas, C. M. *Comments Inorg. Chem.* **2011**, *32*, 14–38. (b) Greenwood, B. P.; Rowe, G. T.; Chen, C.-H.; Foxman, B. M.; Thomas, C. M. *J. Am. Chem. Soc.* **2010**, *132*, 44–45. (c) Thomas, C. M.; Napoline, J. W.; Rowe, G. T.; Foxman, B. M. *Chem. Commun.* **2010**, *46*, 5790–5792. (d) Krogman, J. P.; Foxman, B. M.; Thomas, C. M. *J. Am. Chem. Soc.* **2011**, *133*, 14582–14585. (e) Krogman, J. P.; Bezpalko, M. W.; Foxman, B. M.; Thomas, C. M. *Inorg. Chem.* **2013**, *52*, 3022–3031. (f) Napoline, J. W.; Bezpalko, M. W.; Foxman, B. M.; Thomas, C. M. *Chem. Commun.* **2013**, *49*, 4388–4390. (g) Zhou, W.; Marquard, S. L.; Bezpalko, M. W.; Foxman, B. M.; Thomas, C. M. *Organometallics* **2013**, *32*, 1766–1772. (h) Marquard, S. L.; Bezpalko, M. W.; Foxman, B. M.; Thomas, C. M. *Organometallics* **2014**, *33*, 2071–2079. (i) Wu, B.; Hernández Sánchez, R.; Bezpalko, M. W.; Foxman, B. M.; Thomas, C. M. *Inorg. Chem.* **2014**, *53*, 10021–10023. (j) Wu, B.; Bezpalko, M. W.; Foxman, B. M.; Thomas, C. M. *Chem. Sci.* **2015**, *6*, 2044–2049.
- (7) Krogman, J. P.; Gallagher, J. R.; Zhang, G.; Hock, A. S.; Miller, J. T.; Thomas, C. M. *Dalton Trans.* **2014**, *43*, 13852–13857.
- (8) Marquard, S. L.; Bezpalko, M. W.; Foxman, B. M.; Thomas, C. M. *J. Am. Chem. Soc.* **2013**, *135*, 6018–6021.
- (9) (a) Jeletic, M. S.; Helm, M. L.; Hulley, E. B.; Mock, M. T.; Appel, A. M.; Linehan, J. C. *ACS Catal.* **2014**, *4*, 3755–3762. (b) Jeletic, M. S.; Mock, M. T.; Appel, A. M.; Linehan, J. C. *J. Am. Chem. Soc.* **2013**, *135*, 11533–11536.
- (10) Haumann, M.; Meijboom, R.; Moss, J. R.; Roodt, A. *Dalton Trans.* **2004**, 1679–1686.
- (11) (a) Fang, M.; Wiedner, E. S.; Dougherty, W. G.; Kassel, W. S.; Liu, T.; DuBois, D. L.; Bullock, R. M. *Organometallics* **2014**, *33*, 5820–5833. (b) Wiedner, E. S.; Roberts, J. A. S.; Dougherty, W. G.; Kassel, W. S.; DuBois, D. L.; Bullock, R. M. *Inorg. Chem.* **2013**, *52*, 9975–9988.
- (12) (a) Yu, R. P.; Darmon, J. M.; Milsman, C.; Margulieux, G. W.; Stieber, S. C. E.; DeBeer, S.; Chirik, P. J. *J. Am. Chem. Soc.* **2013**, *135*, 13168–13184. (b) Niu, Q.; Sun, H.; Li, X.; Klein, H. F.; Flörke, U. *Organometallics* **2013**, *32*, 5235–5238. (c) Zhou, H.; Sun, H.; Zhang, S.; Li, X. *Organometallics* **2015**, *34*, 1479–1486.
- (13) (a) Ding, K.; Brennessel, W. W.; Holland, P. L. *J. Am. Chem. Soc.* **2009**, *131*, 10804–10805. (b) Dugan, T. R.; Goldberg, J. M.; Brennessel, W. W.; Holland, P. L. *Organometallics* **2012**, *31*, 1349–1360. (c) Jewson, J. D.; Liable-Sands, L. M.; Yap, G. P. A.; Rheingold, A. L.; Theopold, K. H. *Organometallics* **1999**, *18*, 300–305.
- (14) (a) Cowie, M.; Loeb, S. J.; McKeer, I. R. *Organometallics* **1986**, *5*, 854–860. (b) Frech, C. M.; Shimon, L. J. W.; Milstein, D. *Chem.—Eur. J.* **2007**, *13*, 7501–7509. (c) Zhang, J.; Gandelman, M.; Shimon, L. J. W.; Milstein, D. *Organometallics* **2008**, *27*, 3526–3533.
- (15) (a) Hartwig, J. F. *Angew. Chem., Int. Ed.* **1998**, *37*, 2090–2093. (b) Huang, Z.; Zhou, J.; Hartwig, J. F. *J. Am. Chem. Soc.* **2010**, *132*, 11458–11460.
- (16) (a) Langer, R.; Diskin-Posner, Y.; Leitun, G.; Shimon, L. J. W.; Ben-David, Y.; Milstein, D. *Angew. Chem., Int. Ed.* **2011**, *50*, 9948–9952. (b) Yu, Y.; Sadique, A. R.; Smith, J. M.; Dugan, T. R.; Cowley, R. E.; Brennessel, W. W.; Flaschenriem, C. J.; Bill, E.; Cundari, T. R.; Holland, P. L. *J. Am. Chem. Soc.* **2008**, *130*, 6624–6638.
- (17) Pu, L. S.; Yamamoto, A.; Ikeda, S. *J. Am. Chem. Soc.* **1968**, *90*, 3896–3896.
- (18) (a) Figueroa, J. S.; Cummins, C. C. *J. Am. Chem. Soc.* **2003**, *125*, 4020–4021. (b) Zhu, D.; Korobkov, I.; Budzelaar, P. H. M. *Organometallics* **2012**, *31*, 3958–3971. (c) Erker, G.; Frömberg, W.; Atwood, J. L.; Hunter, W. E. *Angew. Chem., Int. Ed. Engl.* **1984**, *23*, 68–69. (d) Temprado, M.; McDonough, J. E.; Mendiratta, A.; Tsai, Y.-C.; Fortman, G. C.; Cummins, C. C.; Rybak-Akimova, E. V.; Hoff, C. D. *Inorg. Chem.* **2008**, *47*, 9380–9389. (e) Khalimon, A. Y.; Farha, P.; Kuzmina, L. G.; Nikonov, G. I. *Chem. Commun.* **2012**, *48*, 455–457.
- (19) (a) Wakioka, M.; Nakajima, Y.; Ozawa, F. *Organometallics* **2009**, *28*, 2527–2534. (b) Rybin, L. V.; Petrovskaya, E. A.; Rubinskaya, M. I.; Kuz'mina, L. G.; Struchkov, Y. T.; Kaverin, V. V.; Koneva, N. Y. *J. Organomet. Chem.* **1985**, *288*, 119–129. (c) Wakioka, M.; Nagao, M.; Ozawa, F. *Organometallics* **2008**, *27*, 602–608. (d) Esteruelas, M. A.; Lahoz, F. J.; Martín, M.; Martínez, A.; Oro, L. A.; Puerta, M. C.; Valerga, P. *J. Organomet. Chem.* **1999**, *577*, 265–270.
- (20) Chen, C.; Dugan, T. R.; Brennessel, W. W.; Weix, D. J.; Holland, P. L. *J. Am. Chem. Soc.* **2014**, *136*, 945–955.
- (21) (a) Ruddy, A. J.; Sydora, O. L.; Small, B. L.; Stradiotto, M.; Turculeto, L. *Chem.—Eur. J.* **2014**, *20*, 13918–13922. (b) Small, B. L. *Organometallics* **2003**, *22*, 3178–3183. (c) Schmidt, B. *Eur. J. Org. Chem.* **2004**, *2004*, 1865–1880. (d) Seayad, A.; Ahmed, M.; Klein, H.; Jackstell, R.; Gross, T.; Beller, M. *Science* **2002**, *297*, 1676–1678.
- (22) Davis, B. R.; Payne, N. C.; Ibers, J. A. *Inorg. Chem.* **1969**, *8*, 2719–2728.
- (23) Javed, M. I.; Brewer, M. *Org. Lett.* **2007**, *9*, 1789–1792.
- (24) (a) Sur, S. K. *J. Magn. Reson.* **1989**, *82*, 169–173. (b) Evans, D. F. *J. Chem. Soc.* **1959**, 2003–2005.
- (25) *Apex 2*, version 2, User Manual, M86-E01078; Bruker Analytical X-ray Systems: Madison, WI, 2006.